ISSN : 0974 - 7435 Volume 8 Issue 11

BioTechnology
An Indian Journal

FULL PAPER

BTAIJ, 8(11), 2013 [1515-1521]

Contribution of the ion pair R60-D27* to the properties of thermophilic xylose isomerase determined by site-directed mutagenesis

Wei Xu[1], Rong Shao[1]*, Ming Yan[2], Pingkai Ouyang[2]

[1]School of Chemical and Biological Engineering, Yancheng Institute of Technology, Yancheng, (P.R.CHINA)

[2]State Key Laboratory of Materials-Oriented Chemical Engineering, College of Life Science and Pharmacy, Nanjing University of Technology, Nanjing, (P.R.CHINA)

E-mail: sr@ycit.cn

ABSTRACT

The role of ion pair R60-D27* on the subunit interface of *Thermus thermophilus* xylose isomerase was investigated by site-directed mutagenesis and structure analysis. The conserved residue Arg60 in thermophilic xylose isomerases was substituted with hydrophobic residue (Phe) in the mesophilic counterparts. The results show that the maximal specific activity of the mutant V144A/R60F is 32.1 U/mg at 85 °C, which is about 10.46% of V144A, and exhibits an obvious decline in alkaline environment. As to thermostability, after 4 h incubation at 75 °C, the V144A displays about 80% of its initial activity while the mutant V144A/R60F retains only about 50%. Moreover, the catalytic efficiency of mutant V144A/R60F is only 25.34% of that of V144A, which shows an obvious decrease. The structure comparison of V144A and V144A/R60F reveals that the residue D27 shifts slightly outward because of the disruption of ion pair R60-D27*. This affects indirectly the conserved residue F25 which belongs to the active site. The above analysis indicates that the special ion pair R60-D27* plays an important role in keeping the high thermostability, and what's more, it helps to maintain the proper conformation of F25* in the active site of thermophilic xylose isomerases.

KEYWORDS

Xylose isomerase;
Thermus thermophilus;
Site-directed mutagenesis;
Ion pair;
Subunit interface.

INTRODUCTION

Xylose isomerase (XI) (EC 5.3.1.5), widely known as glucose isomerase, catalyses the reversible isomerization of D-xylose to D-xylulose and D-glucose to D-fructose[1]. It plays an essential role in the metabolism of sugars in microorganisms[2-4]. This enzyme is applied to the production of high-fructose corn syrup and continues to be one of the most abundantly applied industrial enzymes. Recently, the utilization of xylose in pretreated and hydrolyzed lignocellulose to produce ethanol becomes a favorite topic[5,6]. The *Saccharomyces cerevisiae* is commonly used for ethanol production. However, it lacks the ability to ferment pentose sugars like D-xylose and L-arabinose[7,8]. Functional expression of a XI in *S. cerevisiae* has long been regarded as the most promising approach to reconstruct *S. cerevisiae* for alcoholic fermentation of D-xylose[9]. Up

to now, several *xyl*A genes encoding XI have been successfully heterologously expressed in *S. cerevisiae*[10-12]. One of them is from *T. thermophilus*[13-15].

The XIs can be divided into two classes according to the homology of amino acid sequences[1]. TthXI is included in Class I, and its structure (PDB ID: 1BXB) was determined by X-ray crystallography[16]. Each monomer of TthXI has 387 residues that is composed of two domains, a catalytic domain (residues 1–321) and a small C-terminal domain (residues 322–387)[16]. The catalytic domain is folded into an $(\alpha/\beta)_8$-barrel and the small domain consists of helices and loops. The active sites that contain two metal cations at the C-terminal end of the barrel[17,18]. C-terminal domain makes extensive contacts with a neighboring subunit resulting in many interactions.

Thermostability as an important characteristic of industrially used enzyme has been paid great attention by the study of thermophilic proteins in comparison with their mesophilic counterparts[19-21]. The Cys306 to Ala mutation within *Streptomyces sp*. SK glucose isomerase dramatically affected its thermal stability by decreasing the half-life, while the Ala63 to Ser replacement increased this half-life[22]. The electrophoretic analysis proves that the residue Cys306 participates in oligomerization of the enzyme.

In comparison with the mesophilic XIs, the decreased cavity volumes and some additional ion pairs on the subunit interfaces of TthXI are considered to contribute to thermostability[16]. The subunit interactions are usually composed of hydrophobic interaction, hydrogen bond and electrostatic attraction of the ion pairs on the interfaces[23-26]. Ion pair interaction is one of the major stabilizing forces for thermostable proteins[27-32]. Chang et al. presented that some of the additional ion pairs located on the subunit interface in TthXI are involved in stabilizing the long loop regions[16]. Asp27 in one subunit forms an ion pair with Arg60 of the Q axis-related subunit in TthXI. It seems that an extra stabilization of long loop regions by ion pairs and ion pair networks including inter-subunit ion pairs contributes to the enhanced thermostability of *Thermus caldophilus* xylose isomerase (TcaXI) and TthXI.

In our previous study, the gene of TthXI was coloned and expressed in *E. coli* BL21 (DE3). Then, it was purified, and its properties were studied in detail[33,34]. The TthXI activity has been enhanced by site-directed mutation on the subunit interfaces. Results show that the specific activities of mutants D375G, K355A and V144A were remarkably increased over a temperature range of 40–90 °C at pH 7.0[35,36]. Our experimental results support the assumption that additional ion pairs formed between R258, E372 and D375 contribute to the enhanced thermostability of thermophilic XIs[16]. We also revealed the effects of temperature on TthXI subunit interactions and residue flexibility by molecular simulation[37]. The B-factors of helix-loop-helix region of involving most of residues 55-80 show large increase at 360 K.

In present work, to reveal the role of ion pair R60-D27* on the subunit interface, the R60F mutation was employed in TthXI which has V144A mutation acquried in previous study[35]. The catalytic properties of the mutant V144A/R60F were investigated, and the possible structural determinants were proposed.

MATERIALS AND METHODS

Chemicals

All reagents were of analytical grade unless otherwise specified and were used as described by the manufacturer. D-xylose was purchased from Sigma (Steinheim, Germany) and sorbitol dehydrogenase (SDH) from Roche (Basel, Switzerland). Restriction endonucleases were purchased from New England Biolabs (MA, USA).

Strains and plasmids

T. thermophilus HB8 was purchased from the German Resource Centre for Biological Material (DSMZ). *Escherichia coli* BL21 (DE3) (F- ompT hsdS (rB- mB-) gal dcm (DE3)) and V144A mutant which was mutated from *T. thermophilus* HB8 XI were stored in our lab[35]. Plasmid pET22b(+) was purchased from Novagen.

Oligonucleotide synthesis and DNA sequencing

PCR primers and mutagenic oligonucleotides (TABLE 1) were synthesized by Shenergy (Shanghai, China). DNA sequences were determined by Bioasia (Shanghai, China).

Site-directed mutagenesis

The R60F mutation was introduced into the V144A gene using the QuickChange® Multi Site-Directed Mutagenesis Kit (Stratagene). For this method the PCR primers are shown in TABLE 1. The mutation in the V144A/R60F was identified by DNA sequencing.

TABLE 1 : Oligonucleotides used for site-directed mutagenesis

Mutations	Oligonucleotides
V144A	5'-AGGGAGCTGAG **GCG**GAGGCCACGGGC-3'
V144A/R60F	5'-ACCTGATCCCG **TTT**GGCACGCCTCCTCAG-3'

Expression of V144A and V144A/R60F in *E. coli* BL21 (DE3)

E. coli BL21 (DE3) harbouring the plasmids pET22b(+) with gene V144A or V144A/R60F was cultured in Luria-Bertani medium containing 100 μg·mL^{-1} ampicillin at 37 °C. Proteins were expressed for 7 h after induction at log phase (A_{600} = 0.6–0.8) by addition of 0.9 mmol·L^{-1} isopropyl β-D-1-thiogalactopyranoside (IPTG)[38]. Then, the cells were harvested by centrifugation and washed once with ice-cold distilled water.

Protein purification

Washed cells were disrupted by sonicating for 5 min (3 s pulse, 5 s interval, 150 W). Cell debris was removed by centrifugation (15, 000 xg for 8 min at 4 °C). The E. coli protein in the supernatant was precipitated by heat treatment (20 min, 75 °C), and then removed by centrifugation. Then the supernatants were purified by an ion-exchange chromatography as described in previous paper[35]. This enzyme preparation was analyzed by Bradford protein and enzymatic activity assays[39], Coomassie blue-stained sodium dodecyl sulate-polyacrylamide gel electrophoresis (SDS-PAGE). Each XI was shown as a single band in SDS-PAGE (Bio-Rad) gel with a molecular mass of about 44 kDa. The enzyme samples were concentrated to 2–6 mg·mL–1 and desalted with Microcon YM-10 centrifugal filter device (Millipore Corporation, Bedford, MA).

Xylose isomerase assays

Xylose isomerase activity was determined by the coupled sorbitol dehydrogenase (SDH) assay as described in the previous paper[35,40].

Biochemical characterization of xylose isomerase

The effect of temperature on enzymatic activity was determined in the reaction mixture at various temperatures ranging from 40 to 90°C.

The effect of pH on enzymatic activity at 60 °C was determined by the routine assay described previously[35] except that the Tris-HCl buffer was substituted with 50 mmol·L–1 sodium acetate (pH 4.9–5.6) and 50 mmol·L–1 Tris-HCl (pH 7.0–9.0). All pH values were adjusted at room temperature.

The kinetic values of K_m, V_{max}, and k_{cat} for the purified recombinant xylose isomerases were measured by the Lineweaver-Burk method. The enzyme activity was tested using D-xylose (ranging from 8–400 mmol·L–1) in 50 mmol·L–1 Tris-HCl buffer (pH 7.5) with 10 mmol·L–1 $MgCl_2$. The molecular weight of 43.9 kDa was used to calculate the catalytic rate constant (k_{cat}) from the relationship $k_{cat} = V_{max}/[E0]$, where [E0] = total enzyme concentration.

Thermal stability was evaluated by measuring xylose isomerase activity after incubation metal-free enzyme preparations in 50 mmol·L–1 Tris-HCl (pH 7.5) in airtight tubes in a heated water bath at 75 °C for various times. At different times, samples were withdrawn and stored on ice. The residual activity was determined at 60 °C as described above.

All xylose isomerase activity determinations were performed in triplicate.

Multiple sequences alignment and the analysis of three-dimensional structure of xylose isomerase

Multiple sequences alignment was performed by Clustal X1.83[41]. The structure of TthXI was got from Protein Data Bank (ID: 1BXB). WHATIF 5.0 was used for homology modeling. Softwares DeepView 3.7[42] and RasMol V2.7[43] were employed to visualize.

RESULTS AND DISCUSSION

Mutation strategy

The residue R60 is conserved in thermophilic bacteria, while the hydrophobic residue (Phe) is conserved

FULL PAPER

in corresponding mesophilic counterparts (Figure 1). The overall 3D structure and mutation position in TthXI are shown in Figure 2. The residue R60 on the subunit interface of TthXI interacts with the residue D27 from an adjacent subunit by forming the ion pair (Figure 3 (a)). The ion pair interaction plays an important role in stabilizing the long loop consisted of residues 18-34. Meanwhile, the residue F25 at the tip of the long loop (residues 18-34) belongs to the active site of the adjacent subunit. Therefore, we can infer that the ion pair R60-D27* may have dual roles. If it is destroyed, both the thermostability and the activity of TthXI will be influenced. The R60→F60 mutation (Figure 3 (b)) disrupts the ion pair interaction between R60 and D27. The protein rigidity might be weakened due to the decreasing of ion pair amounts on subunit interface[35].

Figure 1 : Multiple sequences alignment of Class I XIs by ClustalX 1.83. Mutation sites are marked with rectangles. A: *Actinoplanes missouriensis* (P12851) B: *Ampullariella sp.* (P10654) C: *Arthrobacter sp.* (P12070) D: *Streptomyces albus* (P24299) E: *Streptomyces rubiginosus* (P24300) F: *Streptomyces diastaticus* (P50910) G: *Streptomyces olivaceoviridis* (Q93RJ9) H: *Streptomyces coelicolor* (Q9L0B8) I: *Streptomyces lividans* (Q9RFM4) J: *T. thermophilus* (P26997) K: *Thermus caldophilus* (P56681)

Comparison of properties of V144A with its mutant V144A /R60F

Effects of temperature and pH on the activities V144A and its mutant V144A /R60F

The effects of temperature on the activities of V144A and its mutant V144A/R60F were studied. The specific activity of the mutant V144A/R60F was remarkably decreased over a temperature range of 40 – 90 °C (Figure 4). The maximal specific activity of the mutant V144A/R60F is 32.1 U/mg at 85 °C, which is about 10.46 % of V144A. However, the change in optimum temperature of V144A/R60F was not observed. The effects of pH on the activity of V144A and its mutant V144A/R60F were investigated (Figure 5). In Figure 5, the activity of mutant V144A/R60F exhibits an obvious decline in alkaline environment (pH 8.0–9.0), and is 10.31 % of V144A at pH 7.5.

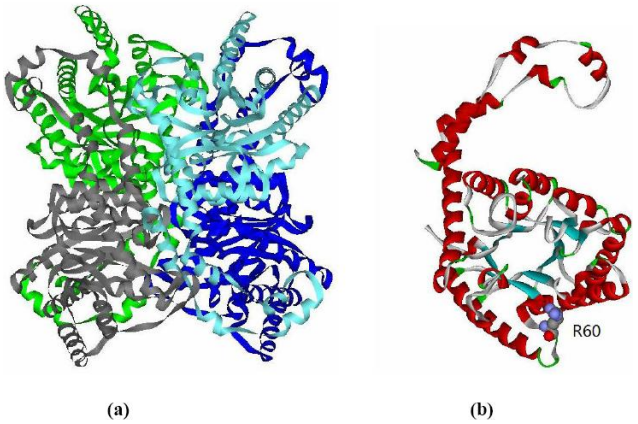

Figure 2 : Structure of TthXI. (a) The 3D-structure of TthXI; (b) The single subunit of TthXI. The residue R60 is the position for mutation

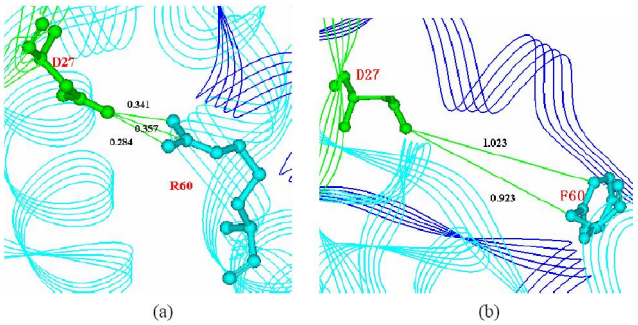

Figure 3 : Three-dimensional model of subunit interactions around mutation site. Subunits A, B, C and D are shown in light blue, green, dark blue and gray, respectively. The distances (nm) between different atoms are shown (a) V144A, The atom-distances of NH2, NH1 and CZ in R60 between OD2 in D27 are 0.284 nm, 0.341 nm and 0.357 nm, respectively. (b) V144A/R60F, Atoms F60 CD and CD1 are 0.923 nm and 1.023 nm from atom D27 OD2.

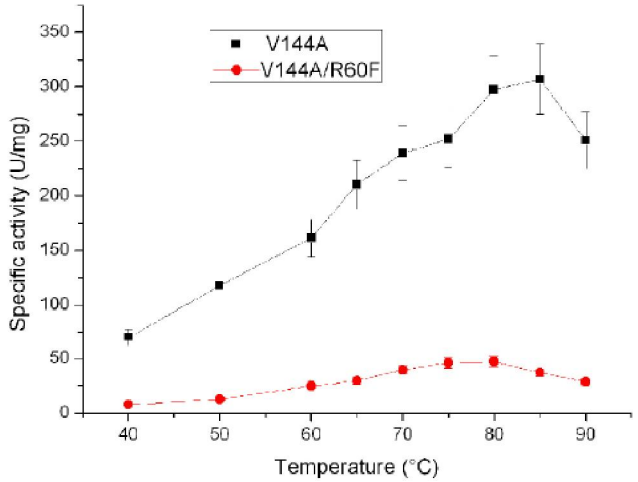

Figure 4 : Effects of temperature on the specific activity of TthXI mutants. (■) V144A; (●) V144A /R60F

Inactivation of the enzyme activity at 75 °C

The residual activities of V144A and its mutant

V144A/R60F were measured after heat treatment at 75 °C in water bath for various lengths of time. It was shown that the thermostability of both V144A and its mutant V144A/R60F was decreased. The V144A exhibited 77% of maximum activity after 4 h of incubation, whilst its mutant V144A/R60F had a more lowered thermostability (Figure 6), only 50.3% of maximum activity. This indicates that introducing R60F mutation in TthXI leads to a decreased thermostability.

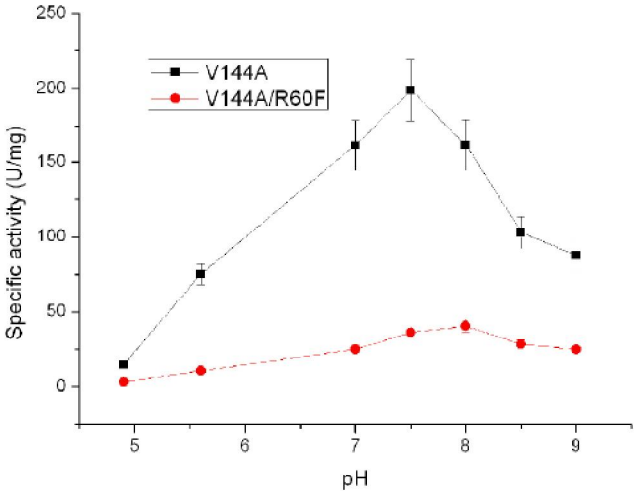

Figure 5 : Effects of pH on the specific activity of TthXI mutants. (■) V144A; (●) V144A /R60F

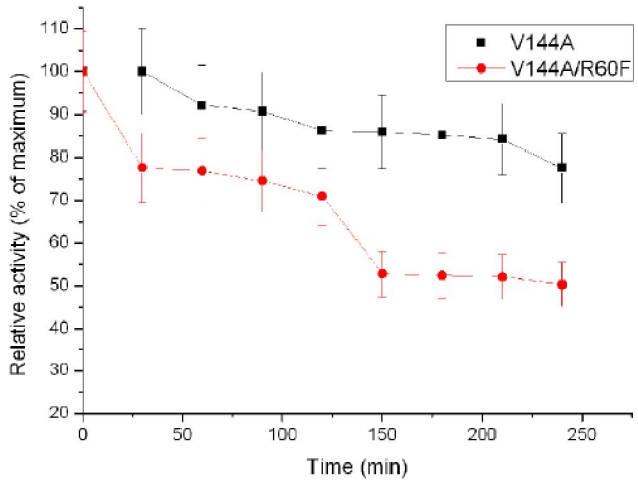

Figure 6. Inactivation graphs of TthXI mutants at 75 °C. (■) V144A; (●) V144A /R60F

Kinetic properties of V144A and its mutant V144A /R60F

The k_{cat}/K_m is the catalytic efficiency that reflects the overall conversion of substrate to product. Kinetic features of the V144A and its mutant V144A/R60F were determined with D-xylose as substrate (TABLE 2). The catalytic efficiency of V144A/R60F shows an obvious decrease, and is 25.34 % of V144A. The result indicates that the R60F mutation alters the catalytic feature of V144A. Kinetic analysis suggests that the decreasing in k_{cat}/K_m ratio of V144A/R60F is caused by a decreased k_{cat} value due to the decline in V_{max}. Meanwhile, the K_m of V144A/R60F shows about 2-fold lower than that of the V144A, meaning a higher affinity for D-xylose. The decrease in k_{cat} also shows that the energy of activation of V144A/R60F has been enhanced compared with V144A.

TABLE 2 : Kinetic parameters of V144A and V144A/R60F

	K_m(mM)	V_{max}(U/mg)	k_{cat} (s^{-1})	k_{cat}/K_m (s^{-1}*mM^{-1})
V144A	27.1 ± 3.4	219.30 ± 20.9	160.48	5.92
V144A/R60F	13.17±1.2	26.93±2.5	19.71	1.50

Analysis the structural mechanism of the mutant V144A/R60F

The results of enzymatic properties show that the activity of mutant V144A/R60F decreases obviously by introducing the single mutation to V144A. Although the residue R60 does not locate at the active site, the ion pair between R60 and D27*(from another subunit) plays an important role in stabilizing the conformation of the long loop (residues 18-34)(Figure 7).

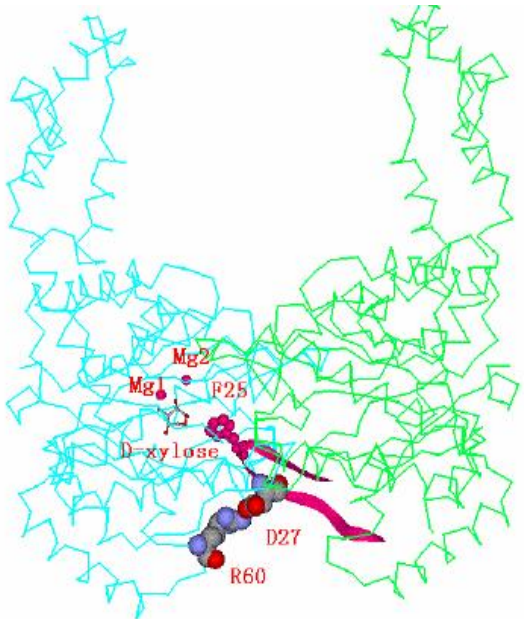

Figure 7 : The location of loop (18-34) in TthXI. Loop (residue 18-34) is shown in red ribbon

FULL PAPER

In order to analyze the structural mechanism of V144A/R60F, the homology model of V144A/R60F was constructed. The structure comparison of V144A and V144A/R60F suggests that the conserved residues (H53, T89, E180 and W136) in the active site show no obvious difference. The residue D27 shifts outward slightly because of the disruption of ion pair R60-D27*. The above change affects the position of residue F25 through residue G26, and the distance between residue F25 and substrate D-xylose is increased. The minor changes in the active site of V144A/R60F may be the main reason to result in the significant decrease in the activity. The above analysis indicates that the special ion pair R60-D27* on the subunit interface of TthXI plays an important role in keeping the high thermostability, what's more, it helps to stabilize the long loop (residue 18-34) to keep the right conformation of F25* in the active site.

The larger conformation change of residue F25 at 360 K was also observed in previous MD simulation [37]. The residue F25 is conserved in all known XIs, and protrudes into the active site of adjacent subunit. The larger conformation change of residue F25 might have an essential role on substrates moving in and out of the active sites.

CONCLUSIONS

Most of studies have focused on enhancement of protein stability by reinforcing the subunit interfaces, whereas the influence of decreasing subunit interactions is barely referred. Ion pair interaction is one of the major stabilizing forces for thermostable proteins. Here, the role of ion pair R60-D27* on subunit interface of *Thermus thermophilus* xylose isomerase was investigated by site-directed mutagenesis and structure analysis. The results show that the maximal specific activity of the mutant V144A/R60F is 32.1 U/mg at 85 °C, which is about 10.46% of V144A, and exhibits an obvious decline in alkaline environment (pH 8.0–9.0). As to thermostability, after 4 h incubation at 75 °C, the V144A displays about 80% of its initial activity while the mutant V144A/R60F retains only about 50%. Moreover, the catalytic efficiency of mutant V144A/R60F is only 25.34% of that of V144A, which shows an obvious decrease. The structure comparison of V144A and V144A/R60F reveals that the residue D27 shifts slightly outward because of the disruption of ion pair R60-D27*. This affects the conserved residue F25 which belongs to the active site, as deduced from the constructed three-dimensional model. The above analysis indicates that the special ion pair R60-D27* locates on the subunit interface of TthXI plays an important role in keeping the high thermostability of TthXI, what's more, it helps to stabilize the long loop(residue 18-34) to maintain the proper conformation of F25* in the active site.

ACKNOWLEDGEMENTS

This study was supported financially by National Natural Science Foundation of China (No. 31101912), the Natural Science Foundation of Jiangsu Province of China (No. BK2011420) and sponsored by Qing Lan Project of Jiangsu Province of China.

REFERENCES

[1] S.H.Bhosale, M.B.Rao, V.V.Deshpande; Microbiol Rev.; **60**, 280–300 **(1996)**.
[2] M.Kuyper, M.J.Toirkens, J.A.Diderich, A.A.Winkler, J.P.van Dijken, J.T.Pronk; FEMS Yeast Research., **9**, 25–34 **(2005)**.
[3] A.J.A.van Maris, A.A.Winkler, M.Kuyper, W.A.M.de Laat, J.P.Dijken, J.T.Pronk; Adv Biochem Engin/Biotechnol. 108 (2007) 179–204.
[4] D.H.Patel, E.J.Cho, H.M.Kim, I.S.Choi,.H.J.Bae, Protein Engineering, Design and Selection., **25**, 331–336 **(2012)**.
[5] B.Hahn-Hägerdal, C.F.Wahlbom, M.Gárdonyi, W.H.van Zyl, O.R.R.Cordero, LJönsson; J. Adv Biochem Eng Biotechnol. 73(2001) 53–84.
[6] G.C.Zhang, J.J.Liu, W.T.Ding; Appl Environ Microbiol., **78**, 1081–1086 **(2012)**.
[7] Y.Wang, W.L.Shi, X.Y.Liu, Y.Shen, X.M.Bao, F.W.Bai; Biotechnol Lett., **26**, 885–890 **(2004)**.
[8] X.L.Liu, N.Jiang, P.He, D.J.Lu, A.Shen; Chinese Science Bulletin., **50**, 653–658 **(2005)**.
[9] S.M.Lee, T.Jellison, H.S.Alper; Appl Environ Microbiol., **78**, 5708–5716 **(2012)**.
[10] G.Márk, H.H.Bärbel; Enzyme Microb Technol., **32**, 252–259 **(2003)**.
[11] D.Brat, E.Boles, B.Wiedemann; Appl Environ Microbiol., **75**, 2304–2311 **(2009)**.

[12] K.H.Dekker, K.Yamagata, S.Sakaguchi; J Bacteriol., **173**, 3078–3083 **(1991)**.

[13] M.Walfridsson, X.M.Bao, M.Anderlund, G.Lilius, L.Bulow, B.Hahn-Hägerdal; Appl Environ Microbiol., **62**, 4648–4651 **(1996)**.

[14] A.Lönn, M.Gárdonyi, W.van Zyl, B.Hahn-Hägerdal, R.C.Otero, Eur J Biochem., **269**, 157–163 **(2002)**.

[15] A.Lönn, K.L.Träff-Bjerre, R.R.C.Otero, W.H.van Zyl, B.Hahn-Hägerdal; Enzyme Microb Technol., **32**, 567–573 **(2003)**.

[16] C.Chang, B.C.Park, D.S.Lee, S.W.Suh; J Mol Biol. **288**, 623–634 **(1999)**.

[17] W.Vangrysperre, J.Vandamme, J.Van de Kerckhove, C.K.Debruyne, R.Cornelis, H.Kerstershilderson; Biochem J., **265**, 699–705 **(1990)**.

[18] A.Y.Kovalevsky, L.Hanson, S.Z.Fisher, M.Mustyakimov, S.A.Mason, V.T.Forsyth, M.P.Blakeley, D.A.Keen, T.Wagner, H.L.Carrell, A.K.Katz, J.P.Glusker, P.Langan; Structure., 18 (2010) 688–699.

[19] D.E.Robertson, B.A.Steer; Curr Opin Chem Biol. **8**, 141–149 **(2004)**.

[20] D.Georlette, B.Damien, V.Blaise, E.Depiereux, V.N.Uversky, C.Gerday; J Biol Chem.; **278**, 37015–37023 **(2003)**.

[21] M.Rahimzadeh, K.Khajeh, M.Mirshahi, M.Khayatian, R.Schwarzenbacher; International Journal of Biological Macromolecules., **50**, 1175–1182 **(2012)**.

[22] M.A.Borgi, M.Rhimi, N.Aghajari, M.B.Ali, M.Juy, R.Haser, S.Bejar, Biologia., **64**, 845–851 **(2009)**.

[23] A.Bashir, R.N.Perham, N.S.Scrutton; Biochem J., **312**, 527–533 **(1995)**.

[24] R.Jaenicke, H.Lilie; Adv Protein Chem., **53**, 329–401 **(2000)**.

[25] R.Thoma, M.Hennig, R.Sterner, K.Kirschner, Structure., **8**, 265–276 **(2000)**.

[26] T.Kabashima, Y.Li, N.Kanada, K.Ito, T.Yoshimoto, Biochim Biophys Acta., **1547**, 214–220 **(2001)**.

[27] S.D'Amico, P.Claverie, T.Collins, D.Georlette, E.Gratia, A.Hoyoux, R.Philos Trans; Soc Lond B Biol Sci, **357**, 917–925 **(2002)**.

[28] V.G.H.Eijsink, A.Bjork, S.Gaseidnes, R.Sirevag, B.Synstad, B.van den Burg, G.Vriend; J Biotechnol. **113**, 105–120 **(2004)**.

[29] I.N.Berezovsky, E.I.Shakhnovich; Proc Natl Acad Sci., **102**, 12742–12747 **(2005)**.

[30] B.C.Bennett, M.Yeager; Structure., **18**, 657 –659 **(2010)**.

[31] L.M.Trevizano, R.Z.Ventorim; S.T.de Rezende; Junior F.P.S., Guimaraes V.M., Journal of Molecular Catalysis B: Enzymatic., **81**, 12–18 **(2012)**.

[32] J.K.Blum, M.D.Ricketts, A.S.Bommarius; Journal of Biotechnology., **160**, 214–221 **(2012)**.

[33] W.Xu, L.Ding, M.Yan, L.Xu; China Biotechnology, **29**, 65–70 **(2009)**.

[34] W.Xu, M.Yan, L.Ding, Y.Li, L.Xu; Computer and Applied Chemistry, **23**, 531–534 **(2006)**.

[35] W.Xu, M.Yan, L.Xu, L.Ding, P.K.Ouyang; Enzyme Microb Tech.; **44**, 77–83 **(2009)**.

[36] R.M.P.Siloto; R.J.Weselake; Biocatalysis and Agricultural Biotechnology., **1**, 181–189 **(2012)**.

[37] W.Xu, P.Cai, M.Yan, L.Xu, P.K.Ouyang; Chinese Journal of Chemical Physics., **22**, 467–472 **(2009)**.

[38] J.Sambrook, E.F.Fristch, T.Maniatis; Molecular Cloning: A Laboratory Manual.,2 rd Edition New York: Cold Spring Harbor Laboratory Press, **(1989)**.

[39] M.M.Bradford; Anal Biochem., **72**, 248–254 **(1976)**.

[40] H.Kerstershilderson, M.Callens, O.Vanopstal, W.Vangrysperre, C.K.Debruyne; Enzyme Microb Technol.; **9**, 145–148 **(1987)**.

[41] D.G.Higgins, P.M.Sharp; Gene., **73**, 237–244 **(1988)**.

[42] N.Guex, A.Diemand, M.C.Peitsch; Trends Biochem Sci., **24**, 364–367 **(1999)**.

[43] R.A.Sayle, E.J.Milner-White; Trends Biochem Sci., **20**, 374–376 **(1995)**.